CIRANO
Allier savoir et décision

Energy Transition Under Mineral Constraints and Recycling

SIMON **CHAZEL**
SOPHIE **BERNARD**
HASSAN **BENCHEKROUN**

2020S-51
CAHIER SCIENTIFIQUE
CS

ISSN 2292-0838 (online version)

Energy Transition Under Mineral Constraints and Recycling *

Simon Chazel †, Sophie Bernard ‡, Hassan Benchekroun §

Abstract/Résumé

What are the consequences of primary mineral constraints on the energy transition? Low-carbon energy production uses green capital, which requires primary minerals. We build on the seminal framework for the transition from a dirty to a clean energy in Golosov et al. (2014) [9] to incorporate the role played by primary minerals and their potential recycling. We characterize the optimal paths of energy transition under various scenarios of mineral constraints. Mineral constraints limit the development of green energy in the long run: low-carbon energy production eventually reaches a plateau. We run our simulations using copper as the limiting mineral and we allow for its recycling. In all our scenarios, we find that allowing for mineral recycling delays by 40-60 years the plateau of green capital. After five to six decades, green energy production is 50% lower than in the benchmark model. GDP is 3-8% lower than in the infinite mineral scenario after 30 decades.

Keywords/Mots-clés: Energy Transition, Green Capital, Recycling, Circular Economy, Mineral Constraint, Dynamic General-Equilibrium Model

---

* Hassan Benchekroun and Simon Chazel thank the Canadian Social Sciences and Humanities Research Council (SSHRC) for financial support.
† Polytechnique Montreal, Department of Mathematics and Industrial Engineering, Canada and Polytechnique Paris, France
‡ Polytechnique Montreal, Department of Mathematics and Industrial Engineering, and CIRANO, Canada
§ McGill University, Department of Economics, and CIREQ, Canada

1 Introduction

The necessity of an energy transition toward low-carbon energy has already been widely documented. However many actors warn that low-carbon energies are more material intensive than fossil energies, so that the energy transition requires huge amounts of raw materials [2].

Low-carbon energy production requires large infrastructures that are made of huge quantities of base metals. Vidal et al. (2013)[24] estimate that "for an equivalent installed capacity, solar and wind facilities require up to [. . . .] 90 times more aluminium, and 50 times more iron, copper and glass than fossil fuels or nuclear energy". Focusing on copper, Hertwich et al. (2015)[10] show that wind and solar energy production technologies are 8 times more copper intensive than coal and oil energy production. Vidal et al. (2013)[24] estimate that the World Wide Fund for Nature (WWF) energy transition scenario requires 40Mt of copper (2 times current annual production) and 310Mt of aluminium (almost 5 times current annual production), which is considerable since renewable energy infrastructures is only a small fraction of those metal use worldwide. Vidal et al. (2017)[25] highlight that those metals production is already highly solicited by many country's current industrialization, and that an energy transition could increase this demand growth to critical levels.

In addition to the scarcity cost, environmental damages of metal mining are substantial, and increase over time when mine depths increases and deposits ore grade declines [18, 12]). Hence, although there is no consensus on the probability of base metals peak production due to resource exhaustion in the next centuries[3], the aim of a circular economy (100% of green capital input coming from recycled mineral) implies to limit primary resource mining to a certain level. Even in the hypothetical case of abundant resources, growing environmental constraints call for a decline of primary resource production.

Base metals have a very high recycling potential, and recycling industry are already developed and cost efficient. For example, recycled copper has the exact same physical properties and value as primary copper, and one fifth of world copper production already comes from recycling. Metal recycling is also

[2] See, for instance, [22, 21, 1, 6, 7]

[3] See, for instance, [18, 16, 20] for the discussion on this topic.

in general 50-90% more energy-efficient than primary production. However, secondary mineral production is limited by the total amount of mineral that has first been mined, so that recycling in itself can not sustain a growing demand. Even with high recycling potential, we rely on primary mineral production to match the booming demand for minerals.

In this paper, we examine the impact of limited mineral availability on energy transition. We build on the seminal framework developed in Golosov, Hassler, Krussel and Tsyvinski (2014)[9], GHKT. In that model, carbon-free energy production only depends on labor inputs: they abstract from mineral resources constraints. We show how a limited access to mineral resources affects GHKT core results on the energy transition. Using copper as the mineral input in low-carbon energy production, we run simulations under various scenarios of physical and recycling constraints. In all scenarios, we find that the mineral constraint limits the development of green energy: in our model green energy eventually reaches a plateau, in contrast with GHKT where it grows at a positive rate in the long-run. Our simulations also provide insights into the 'mineral transition', from primary extraction to recycling in green capital constitution. Mineral recycling delays by 40-60 years the green capital plateau. In the following decades, labour productivity gains compensate this plateau, but green energy production growth rate drops. After 6-8 decades, green energy production reaches a peak.

Section 2 covers the model. In section 3 we characterize the optimal paths of labour allocations across sectors as well as the the resources scarcity rents. Section 4, covers the simulation method and the model's calibration. In section 5, we highlight the insights learned from a series of six specific results. In section 6 we conduct a robustness check with respect to the low-carbon energy production function. Section 7 concludes.

2 The model

2.1 Equations

We follow closely the architecture of GHKT's model, and build up on that framework to include the production function of the green energy, the green capital and the dynamics of the mineral sector. This is specified in in section 2.1.1 below.

2.1.1 GHKT (2014)

The simulation lasts T periods and the discount factor is denoted by β .

Denote by C_t the consumption, and $U(C_t)$ the instant utility of a representative household

$$U(C_t) = \ln(C_t). \tag{1}$$

Denote by Y_t the total output of the economy, and K_t the amount of capital. In each period, the production of final goods is shared between immediate consumption (C_t) and savings (i.e. constituting capital for the next period). A total depreciation of capital over the course of one period is assumed. Therefore,

$$K_{t+1} + C_t = Y_t \tag{2}$$

$$0 \leq C_t \leq Y_t. \tag{3}$$

Final goods are produced from capital K_t, labour $N_{0,t}$ (where 0 stands for final good sector), and energy E_t. The production function is a standard Cobb-Douglas function:

$$Y_t = A_{0,t}\ e^{-\gamma(S_t-\bar{S})}\ K_t^{\alpha}\ N_{0t}^{1-\alpha-\nu}\ E_t^{\nu}. \tag{4}$$

$A_{0,t}$ is the total factor productivity, α and ν are the output elasticities of capital and energy. Production of final goods also depends on climate (described here by the amount of carbon in the atmosphere S_t), with a damage factor γ. $\bar{S}$ is the preindustrial level of atmospheric carbon.

Energy comes from three sources : oil ($E_{1,t}$), coal ($E_{2,t}$) and a low-carbon energy ($E_{3,t}$). Those sources of energy are imperfect substitutes. The parameter ρ characterizes interfuel substitution. The share parameters κ_1, κ_2 and κ_3 characterizes the relative efficiency of each energy sources:

$$E_t = (\kappa_1 E_{1,t}^{\rho} + \kappa_2 E_{2,t}^{\rho} + \kappa_3 E_{3,t}^{\rho})^{\frac{1}{\rho}}. \tag{5}$$

Oil is extracted from the oil stock $R_{1,t}$. The cost of extraction, in terms of labour, capital and energy, is assumed to be negligible with respect to the cost of scarcity. Therefore, $E_{1,t}$ can be chosen freely in the range of admissible values, without any labour, capital or energy involved.

$$E_{1,t} = R_{1,t} - R_{1,t+1} \tag{6}$$

$$0 \leq E_{1,t} \leq R_{1,t}. \tag{7}$$

As an abundant resource, coal's extraction cost dominates its scarcity cost. Therefore, GHKT assumes an extraction cost :

$$E_{2,t} = A_{2,t} N_{2,t}, \tag{8}$$

where $A_{2,t}$ is an exogenous labour productivity variable.

Carbon emissions accumulates in the atmospheric carbon stock at each period. In the same time, this stock depreciates. Denote $(d_s)_{s=0}^{\infty}$ the proportions of CO2 emitted s periods ago that have been removed from the atmosphere. GHKT specifies the sequence $(d_s)_{s=0}^{\infty}$. Then,

$$S_t = S_{t=0} + \sum_{s=0}^{t} (1 - d_s)\ (E_{1,t-s} + E_{2,t-s}). \tag{9}$$

2.1.2 Green Capital and Minerals

Unlike GHKT, we make capital a crucial production factor of low-carbon energy production. Following Fabre et al. (2020), we refer to this capital as *green capital*, and denote it G_t. To produce low-carbon energy, one needs labour $N_{3,t}$ and green capital G_t. We use a standard CES production function with a negative parameter of substitution $\ddot{\rho}$. $A_{3,t}$ measures labour productivity. It is an exogenous variable. Parameter ψ characterizes the energy that can be obtained from a given amount of green capital over the course of one period. The variable $N_{3,t}$ stands for labour directly involved in low-carbon energy production:

$$E_{3,t} = (\kappa_L (A_{3,t} N_{3,t})^{\ddot{\rho}} + \kappa_G (\psi G_t)^{\ddot{\rho}})^{\frac{1}{\ddot{\rho}}}. \tag{10}$$

Green capital G_t is constituted from primary and secondary mineral resources. Denote $m_{p,t}$ (resp. $m_{s,t}$) the flow of primary (resp. secondary) mineral. Green capital production function is a standard CES function. The substitution parameter of primary and secondary mineral resources is $\tilde{\rho}$, and the share parameters are κ_s and κ_p. As for regular capital in GHKT, a total depreciation of green capital is assumed over the course of one period. Thus, it depends on the current flow of primary and secondary mineral, and does not depend on the past amount of green capital:

$$G_t = (\kappa_s m_{s,t}^{\tilde{\rho}} + \kappa_p m_{p,t}^{\tilde{\rho}})^{\frac{1}{\tilde{\rho}}}. \tag{11}$$

Primary mineral is extracted from a primary mineral stock $M_{p,t}$. As for coal in GHKT, primary mineral extraction requires labour, which productivity is $A_{p,t}$. Primary mineral extraction is bounded by remaining primary mineral reserves.

$$m_{p,t} = A_{p,t} N_{p,t} \tag{12}$$

$$m_{p,t} \leq M_{p,t} \tag{13}$$

$$M_{p,t+1} = M_{p,t} - m_{p,t}. \tag{14}$$

Similarly, secondary mineral extraction requires a labour input, which productivity is denoted by the exogenous variable $A_{s,t}$. It is bounded by the total reserve of secondary mineral available at this time.

$$m_{s,t} = A_{s,t} N_{s,t} \tag{15}$$

$$0 \leq m_{s,t} \leq M_{s,t}. \tag{16}$$

Since green capital depreciates entirely over the course of one period, secondary mineral stock evolution is :

$$M_{s,t+1} = M_{s,t} - m_{s,t} + (m_{s,t} + m_{p,t})$$

which gives

$$M_{s,t+1} = M_{s,t} + m_{p,t}. \tag{17}$$

It is assumed, as in GHKT, that labour can move freely between all sectors from one period to another. The only feasibility constraint on labour allocation is

$$N_{0,t} + N_{2,t} + N_{3,t} + N_{p,t} + N_{s,t} = N_t \tag{18}$$

with N_t the total labour, that is exogenously driven.

3 The planner's problem

The social planner's problem is to maximize the total discounted utility,

$$\max_{\{C_t,K_{t+1},N_{0,t},E_{1,t},N_{2,t},N_{3,t},N_{p,t},N_{s,t}\}_{t=0}^{\infty}} \sum_{t=0}^{\infty} \beta^t U(C_t)$$

under the feasibility constraints (2), (3), (7), (13), (16), (18). The constraints are linear, and the objective function is strictly concave, so that there is a unique solution to the optimisation problem. Note that the problem's number of decision variables was reduced to eight,i.e., C_t, K_{t+1}, $N_{0,t}$, $E_{1,t}$, $N_{2,t}$, $N_{3,t}$, $N_{p,t}$ and $N_{s,t}$. All the other variables can be obtained as a combination of these eight variables, using equations (4)-(6), (8)-(12), (14)-(15), (17).

3.1 Lagrangian

We write the Lagrangian, using Greek letters for the Lagrange multipliers. We voluntarily omit the Karush-Kuhn-Tucker multipliers here for readability purposes.

$$
\begin{aligned}
\mathcal{L} = \sum_{t=0}^{T} \beta^t U(C_t) &+ \sum_{t=0}^{T} \beta^t \pi_{K,t}\ (K_{t+1} - Y_t + C_t) \\
&+ \sum_{t=0}^{T} \beta^t \lambda_{0,t}\ (Y_t - A_{0,t}\ exp^{-\gamma_t(S_t-\bar{S})}\ K_t^{\alpha}\ N_{0,t}^{1-\alpha-\nu}\ E_t^{\nu}) \\
&+ \sum_{t=0}^{T} \beta^t \xi_t\ (E_t - (\kappa_1 E_{1,t}^{\rho} + \kappa_2 E_{2,t}^{\rho} + \kappa_3 E_{3,t}^{\rho})^{\frac{1}{\rho}}) \\
&+ \sum_{t=0}^{T} \beta^t \mu_{1,t}\ (E_{1,t} - R_{1,t} + R_{1,t+1}) \\
&+ \sum_{t=0}^{T} \beta^t \lambda_{2,t}\ (E_{2,t} - A_{2,t} N_{2,t}) \\
&+ \sum_{t=0}^{T} \beta^t \zeta_t\ (S_t - \bar{S} - \sum_{s=0}^{t+T_0} (1-d_s)\ (E_{1,t-s} + E_{2,t-s})) \\
&+ \sum_{t=0}^{T} \beta^t \lambda_{3,t}\ (E_{3,t} - (\kappa_L (A_{3,t} N_{3,t})^{\ddot{\rho}} + \kappa_G (\psi G_t)^{\ddot{\rho}})^{\frac{1}{\ddot{\rho}}}) \\
&+ \sum_{t=0}^{T} \beta^t \pi_{G,t}\ (G_t - (\kappa_s m_{s,t}^{\tilde{\rho}} + \kappa_p m_{p,t}^{\tilde{\rho}})^{\frac{1}{\tilde{\rho}}}) \\
&+ \sum_{t=0}^{T} \beta^t \lambda_{p,t}\ (m_{p,t} - A_{p,t} N_{p,t}) \\
&+ \sum_{t=0}^{T} \beta^t \mu_{p,t}\ (M_{p,t+1} - M_{p,t} + m_{p,t}) \\
&+ \sum_{t=0}^{T} \beta^t \lambda_{s,t}\ (m_{s,t} - A_{s,t} N_{s,t}) \\
&+ \sum_{t=0}^{T} \beta^t \mu_{s,t}\ (M_{s,t+1} - M_{s,t} - m_{p,t}) \\
&+ \sum_{t=0}^{T} \beta^t \chi_t^N\ (N_{0,t} + N_{2,t} + N_{3,t} + N_{p,t} + N_{s,t} - N_t).
\end{aligned}
$$

We derive analytically the optimal path of the allocation of labor across sectors and 3.3 presents a set of conditions that characterize the optimal paths of the scarcity rents of resources stocks. Section 3.4 gives a necessary condition on labour productivities initial values $A_{s,t=0},\ A_{p,t=0},\ A_{3,t=0}$ that, when the mineral stock is infinite, the planner's solution in our model corresponds to the planner's solution in GHKT.

3.2 Labour distribution in optimal paths

Labour force is shared between five sectors : final goods, coal extraction, low-carbon energy, primary and secondary mineral. In each sector, it contributes to final goods production, either directly ($N_{0,t}$), or indirectly via energy production ($N_{2,t}$, $N_{3,t}$, $N_{s,t}$, $N_{p,t}$). Using the Lagrangian, we prove that the optimal distribution of labour, when feasibility constraint (16) is not binding, is achieved when marginal benefit of labour in each sector is equal.

Proposition 1 *In the optimal paths, marginal benefit of labour in each sector is equal at all time. More specifically, coal labour's marginal benefit is equated to final good's labour marginal benefit:*

$$\frac{\partial Y_t}{\partial N_{0,t}} = \frac{\partial Y_t}{\partial E_t}\frac{\partial E_t}{\partial E_{2,t}}\frac{\partial E_{2,t}}{\partial N_{2,t}} - \Lambda_t \frac{\partial E_{2,t}}{\partial N_{2,t}} \tag{19}$$

where Λ_t *is the optimal tax ratio defined in GHKT.*
Marginal benefit of direct labour in low-carbon energy production is equated to marginal benefit of labour in final good's sector:

$$\frac{\partial Y_t}{\partial N_{0,t}} = \frac{\partial Y_t}{\partial E_t}\frac{\partial E_t}{\partial E_{3,t}}\frac{\partial E_{3,t}}{\partial N_{3,t}}. \tag{20}$$

When the feasibility constraint (16) *is not binding, marginal benefit of labour in mineral recycling and in final good's sector are equal:*

$$\frac{\partial Y_t}{\partial N_{0,t}} = \frac{\partial Y_t}{\partial E_t}\frac{\partial E_t}{\partial E_{3,t}}\frac{\partial E_{3,t}}{\partial G_t}\frac{\partial G_t}{\partial m_{s,t}}\frac{\partial m_{s,t}}{\partial N_{s,t}}. \tag{21}$$

A proof of Proposition 1 is available in appendix B.

Notice that coal extraction contributes to welfare both via final good production and via climate externality. The positive contribution corresponds to the first term of the right-hand side in equation 19. The negative contribution to welfare, via the climate externality, corresponds to the second term.

When the recycling feasibility constraint (16) is binding, that is

$$M_{s,t} = A_{s,t}N_{s,t},$$

the Karush-Kuhn-Tucker multiplier associated to this equation in the Lagrangian is non-null. Therefore, a supplementary term appears when writing the first order condition with respect to $N_{s,t}$, and equation (21) does not hold anymore. However, in this situation, $N_{s,t}$ can be directly obtained from :

$$N_{s,t} = \frac{M_{s,t}}{A_{s,t}}.$$

Notice that primary mineral sector's labour contributes to welfare both directly (via the primary mineral flow $m_{p,t}$) and indirectly (via the constitution of the secondary mineral stock $M_{s,t}$ and depletion of primary mineral stock $M_{p,t}$). Therefore, labour in primary mineral sector contributes to both present and future welfare, so that its marginal contribution to total welfare can not be written explicitly, contrary to other sectors labour's welfare marginal contributions.

3.3 Stock resources scarcity rent variation in optimal paths

We derive from the Lagrangian two more optimality conditions, that goes back to Hotelling's result : stock resources scarcity rent increases at the discount rate. This result holds for both oil and mineral sectors. Proposition 2 specifies this result. A proof is given in appendix C.

Proposition 2 *In the optimal paths, stock resources scarcity rent increase at rate $\frac{1}{\beta}$. For oil stock, we have :*

$$\left(\frac{\nu\kappa_1}{E_{t+1}^{\rho}E_{1,t+1}^{1-\rho}} - \widehat{\Lambda}_{t+1}\right) = \frac{1}{\beta}\left(\frac{\nu\kappa_1}{E_t^{\rho}E_{1,t}^{1-\rho}} - \widehat{\Lambda}_t\right). \tag{22}$$

For primary and secondary mineral stocks, we have :

$$\left(\kappa_p\pi_{G,t+1}\left(\frac{G_{t+1}}{m_{p,t+1}}\right)^{1-\tilde{\rho}} - \frac{1-\alpha-\nu}{A_{p,t+1}N_{0,t+1}}\right) = \frac{1}{\beta}\left(\kappa_p\pi_{G,t}\left(\frac{G_t}{m_{p,t}}\right)^{1-\tilde{\rho}} - \frac{1-\alpha-\nu}{A_{p,t}N_{0,t}}\right) \tag{23}$$

where $\pi_{G,t}$ is the marginal contribution of green capital to welfare

$$\begin{aligned}\pi_{G,t} &= U'(C_t)\frac{\partial Y_t}{\partial E_t}\frac{\partial E_t}{\partial E_{3,t}}\frac{\partial E_{3,t}}{\partial G_t} \\ &= -\frac{Y_t}{C_t}\frac{\nu\kappa_3\kappa_G\psi}{E_t}\left(\frac{E_t}{E_{3,t}}\right)^{1-\rho}\left(\frac{E_{3,t}}{\psi G_t}\right)^{1-\ddot{\rho}}\end{aligned}$$

and $\widehat{\Lambda}_t = \frac{\Lambda_t}{Y_t}$.

Equation (22) gives a condition that links $E_{1,t}$ to $E_{1,t+1}$. It is identical to GHKT's result. Equation (23) links $N_{p,t}$ to $N_{p,t+1}$. It is specific to our model.

3.4 Relationship to the benchmark model (GHKT)

We find the proper calibration of parameters, such that our model's infinite mineral scenario is identical to GHKT's model, in which there is no mineral constraint. In the next paragraphs, we identify GHKT variables with a $\sim$ to differentiate with our model's variable. Moreover, growth rates of labour productivity A_i is denoted g_{Ai}.

In GHKT, renewable energy production function is

$$\widetilde{E}_{3,t} = \widetilde{A}_{3,t}\widetilde{N}_{3,t}$$

where labour productivity $\widetilde{A}_{3,t}$, follows the exogenous paths defined by

$$\begin{cases} \widetilde{A}_{3,t+1} = \widetilde{g}_{A3} \times \widetilde{A}_{3,t} \ \textit{where} \\ \widetilde{A}_{3,t=0} = 1311 \\ \widetilde{g}_{A3} = 1.02^{10}. \end{cases}$$

Proposition 3 below, clarifies the conditions under which we generate GHKT's optimal paths as a particular case of our model where the amount of mineral is infinite.

Proposition 3 *Assume that $M_{p,t=0} = M_{s,t=0} = +\infty$.*
There exists a function F such that when

$$\begin{cases} g_{A3} = g_{As} = g_{Ap} = \widetilde{g}_{A3} \\ \widehat{A}_{3,t=0} \equiv F(A_{3,t=0},\ A_{s,t=0},\ A_{p,t=0}) = \widetilde{A}_{3,t=0} \end{cases}$$

(see appendix D for details on the function F), we have,

- *total labour in low-carbon energy production (direct and indirect) is shared in constant proportion between the three sectors* $N_{3,t}$*,* $N_{p,t}$ *and* $N_{s,t}$

- *low-carbon energy production function can be written as the product of an aggregated low-carbon labour productivity* $\widehat{A}_{3,t}$ *times aggregated low-carbon energy labour* $N_{3,t} + N_{s,t} + N_{p,t}$

- *this aggregated labour productivity* $\widehat{A}_{3,t}$ *has the same initial value and growth rate as GHKT's low-carbon labour productivity.*

Mathematically:
$\forall t \geq 0$,

$$E_{3,t} = \widehat{A}_{3,t}(N_{3,t} + N_{s,t} + N_{p,t}) \quad (24)$$

$$\frac{N_{p,t}}{N_{s,t}} = \alpha_1 \quad (25)$$

$$\frac{N_{3,t}}{N_{s,t} + N_{p,t}} = \alpha_2 \quad (26)$$

$$(27)$$

with

$$\begin{cases} \widehat{A}_{3,t=0} = 1311 \\ \widehat{g}_{A3} = 1.02^{10}. \end{cases}$$

Appendix D provides a proof of proposition 3, and detailed expressions of aggregated labour productivity $\widehat{A}_{3,t=0}$ and labour share ratios expressions α_1 and α_2.

Proposition 1 and Proposition 2 are used for the numerical resolution of the model while Proposition 3 is used for the calibration of the model.

4 Simulations

Section 4.1 details the method used for the simulations. Section 4.2 provides the details of the calibration of the model.

4.1 Method

The simulation is made on Matlab. Following GHKT, we compute an approximate finite horizon solution, with a 300 years horizon, that is 30 periods of 10 years. As in GHKT, the consumption level is a constant ratio of total output Y_t. Constraints (2) and (18) allow to eliminate 2 more decisions variables, for instance K_{t+1} and $N_{0,t}$. At this point, 5 decisions remain in each period: labour distribution N_2, N_3, N_s, N_p, and primary mineral extraction level E_1. Since the simulation lasts 30 periods, there is a total of 150 decisions.

We use propositions 1 and 2 to reduce the problem to a two variable optimisation problem. First, proposition 1 allows to compute $N_{2,t}$, $N_{3,t}$ and $N_{s,t}$, when $N_{p,t}$ and $E_{1,t}$ are given by solving a non-linear 3 equation system. Then, proposition 2 allows to deduce the optimal $N_{p,t+1}$ and $E_{1,t+1}$ when $N_{p,t}$ and $E_{1,t}$ are given, by solving a non-linear 2 equations system. Both of those systems are solved using *fsolve*. In the end, for any duplet of initial values ($E_{1,t=0}$, $N_{p,t=0}$), we are able to compute the paths that:

- start with the given initial values for $E_{1,t}$ and $N_{p,t}$
- respect optimality conditions given in propositions 1 and 2
- respect all feasibility conditions

Finally, we optimise on those two initial values to maximise the total discounted value, using *fminsearch*.

4.2 Calibration

For every parameter that already exists in GHKT, we use the same values than the benchmark model. Then, we calibrate the parameters that are specific to our model using the case of copper in wind energy production. Values are given in Table 1, and appendix A gives more detail on the calibration conditions used. The next paragraph details the various mineral constraint scenarios studied here.

Primary mineral initial stock $M_{p,t=0}$ There is no consensus in the literature in the estimation of total copper resources ultimately available for mining. Indeed, although there are more than 100Mt of copper in the top kilometers of earth crust, most of deposits have such a low ore grade, or are located so deep that it is not technically possible or economically viable to recover it.

The commonly used notion of resource does not include all those deposits, but only those that have reasonable prospect for economic extraction [3]. As a consequence, resources estimates depend on many economic parameters, and

Table 1: Parameter selection

Parameter	Value	Unit
κ_s (κ_p)	0.3085 (0.6915)	-
$\tilde{\rho}$	0.5	-
$A_{p,t=0}$	132000	MtCu/labour
$A_{s,t=0}$	132000	MtCu/labour
ψ	1.877	Gtoe/MtCu
κ_g (κ_L)	0.75 (0.25)	-
$\ddot{\rho}$	-3	-
$A_{3,t=0}$	865.1	Gtoe/labour
$g_{A2} = g_{A3} = g_{As} = g_{Ap}$	1.02^{10}	-
$M_{s,t=0}$	19	MtCu

can change if extraction costs are reduced, or if technological innovations grants (economically viable) access to further deposits. Thus, US Geological Survey identified world copper resource estimation have increased fourthfold between 1998 and 2014, from 550MtCu to 2100MtCu [14, 23]. However, it is unclear if technological innovations and productivity gains can maintain on the long run constant copper extraction cost while deposits inevitably become poorer and more remote. In other words, as Meinert et al. (2016) highlights, it is hard to provide an estimate of ultimate recoverable resource. Moreover, our model only consider one specific use of copper, that is the manufacturing of green capital for low-carbon energy production. However, copper production is dedicated to many different uses, that are not accounted for in this model. Therefore, only a small ratio of total copper resources will be used for green capital manufacturing. This is an additional difficulty in the calibration of the initial stock of copper in our model.
Finally, we argue that in a sustainable development perspective, environmental damages caused by booming primary metal mining makes it relevant to consider a primary mineral constraint lower than ultimate available resources. Indeed, mining is one of the top polluting industry [19] [25]. Additionally, the inevitable ore grade decline tends to increase environmental damages, since more material have to be removed from the mine to recover the same copper amount [18].

For all those reasons, our model's initial primary copper stock has to be understood as a copper budget for energy transition (analog to the carbon budget notion) rather than ultimate recoverable resources. It is an upper limit of copper available for green capital manufacturing, which level depends both on global copper scarcity hypothesis and on environmental degradation mitigation goals. We model various scenarios of copper budget for wind energy production, from 50MtCu (2.5 year of current annual copper primary production, and 20 times the current amount of copper used in wind turbines worldwide) to a very liberal 2000MtCu (recall that current estimate of total copper resources, identified and undiscovered, is 5000Mt).

5 Results

This section presents the results of the set of simulations performed. They are the first best solution to the social planner's problem. As in GHKT, we use in the simulation a time unit of 10 years : for instance, t=10 stands for year 2110 (time starts in 2010).

In the infinite mineral scenario, there is no scarcity rent for primary and secondary minerals. We prove that low-carbon energy production function can be written as the product of a labour share times an aggregated labour productivity. We calibrate our model so that this aggregated labour productivity matches GHKT low-carbon energy labour's productivity. Figure 1 shows the low-carbon energy path in both simulations, GHKT's and ours. There is less than 1% relative error. The results are analog or better for every other variables.

This is an important consistency check, since we intend to measure the impact of a mineral constraint on the optimal energy transition paths computed by GHKT.

5.1 Low-carbon energy production

When there is a finite amount of mineral in the model, primary and secondary mineral flows are bounded. Therefore, green capital is also bounded. However low-carbon energy is produced with labour and green capital inputs. Since the parameter capturing labour-capital substitution is negative, the upper limit on green capital induces an upper limit on low-carbon energy production. Therefore, the mineral constraint leads to a limitation on low-carbon energy production.

Figure 2 shows low-carbon energy production paths under various mineral stock scenarios. In the infinite mineral scenario, production grows unlimited

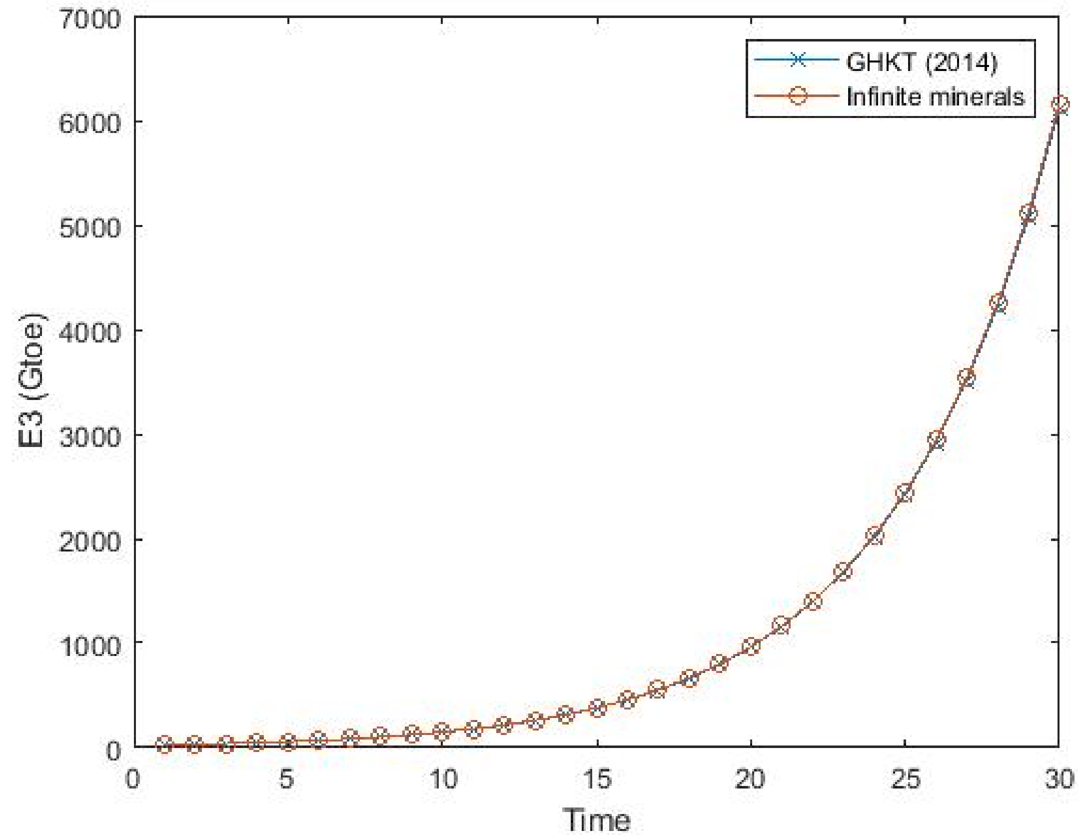

Figure 1: Comparison of low-carbon energy production in GHKT and our model's infinite mineral scenario

at a yearly growth rate of 1.9%. At the end of time horizon, when the mineral stock is finite, the low-carbon energy is just a fraction of its value under resource abundance: less than 10% even in the scenario with $\boldsymbol{M_{p,0}}$=2000 MtCu. For the three scenarios with initial stocks of copper $M_{p,0}$ = 50, 100, 200 MtCu, the paths of low-carbon energy production is notably below the low-carbon energy path under unconstrained mineral availability, from the initial period.

Result 1 *Under a primary mineral constraint scenarios, low-carbon energy production reaches a peak, which date and value depends on total mineral amount.*

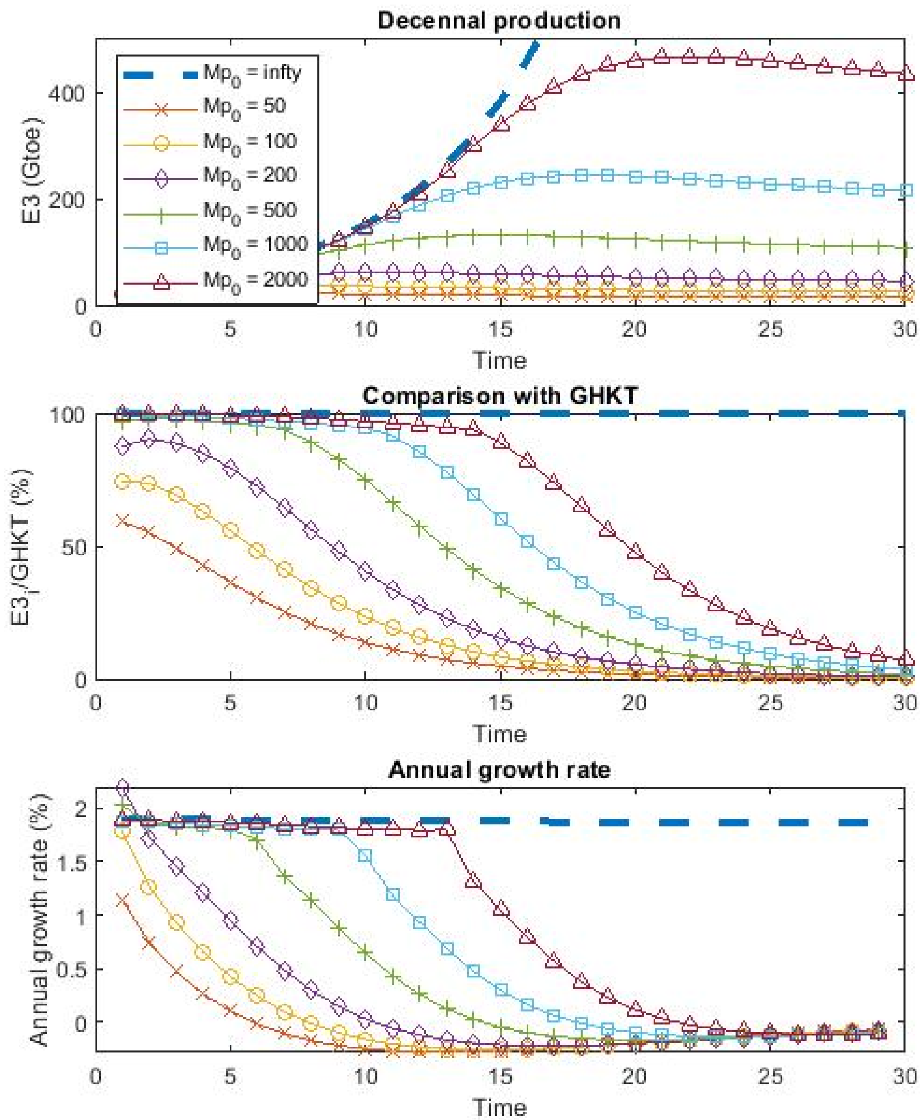

Figure 2: Low-carbon energy production in various mineral stock scenario

5.2 Primary and secondary copper production

Figure 3 shows primary copper extraction paths in all scenarios. In the infinite mineral scenario, primary copper extraction grows by 1.9% annually. In all other scenarios, primary copper production peaks in the next century. In the 3 scenarios with the hardest primary mineral constraint ($M_{p,0} = 50,\ 100,\ 200$ MtCu), the peak happens at the first period of the simulation.

After the primary copper production peaks, recycled copper production growth increases to compensate for the decline of primary copper. The recycling rate (defined here as the ratio of the secondary mineral stock that is recycled in a given period) increases, until it reaches its maximum of 100%, which takes 4-6 decades. Once this maximum is reached, green capital can not increase anymore. This moment coincides with the low-carbon energy production growth drop. Therefore, we conclude that mineral recycling delays the peak of green energy production by 40-60 years.

Result 2 *After the primary mineral extraction peak, mineral recycling increases, which delays by 40-60 years the green energy production growth drop. This delay does not depend on the total amount of mineral in the model.*

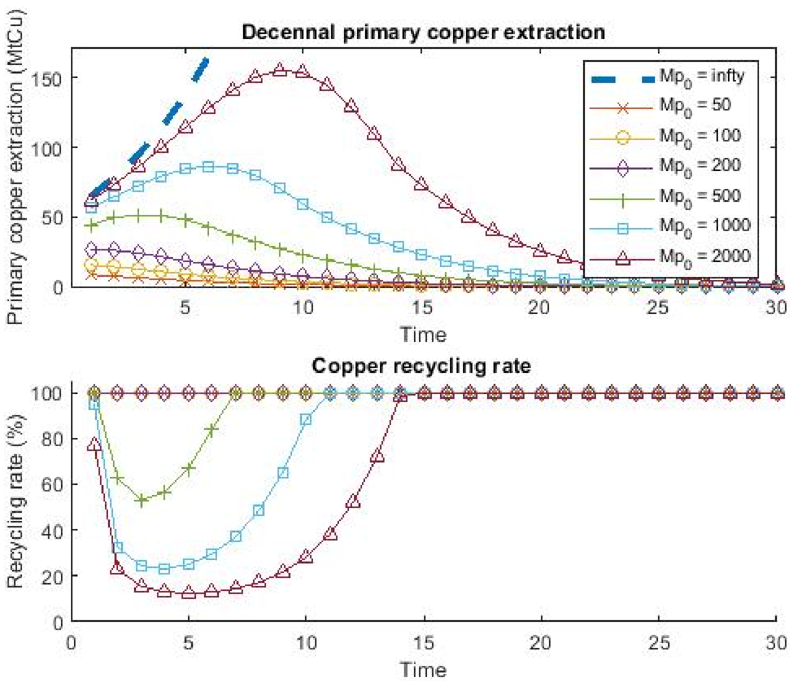

Figure 3: Decennal primary copper extraction m_p, and copper recycling rate paths in all scenarios

5.3 Green capital recycled mineral content

Green capital is made of primary and secondary minerals. Figure 4 shows the evolution of the recycled mineral ratio in green capital manufacturing. In the infinite mineral scenario, this ratio is constant at 15%. In all other scenarios, recycled mineral gradually substitutes to primary mineral in green capital manufacturing. Within 10 to 12 decades, the share of recycled mineral in green capital increases from 20% to 90%. In the long run, green capital is made of 100% recycled minerals. A comparison between Figure 3 and Figure 4 shows that recycled mineral share in green capital starts to increase before primary mineral production peak, when primary mineral production growth starts to slow down and depart from the infinite mineral scenario. When primary mineral production peak occurs (Figure 3), the recycled mineral content of green capital has already reached 55% (± 5%) in all scenarios.

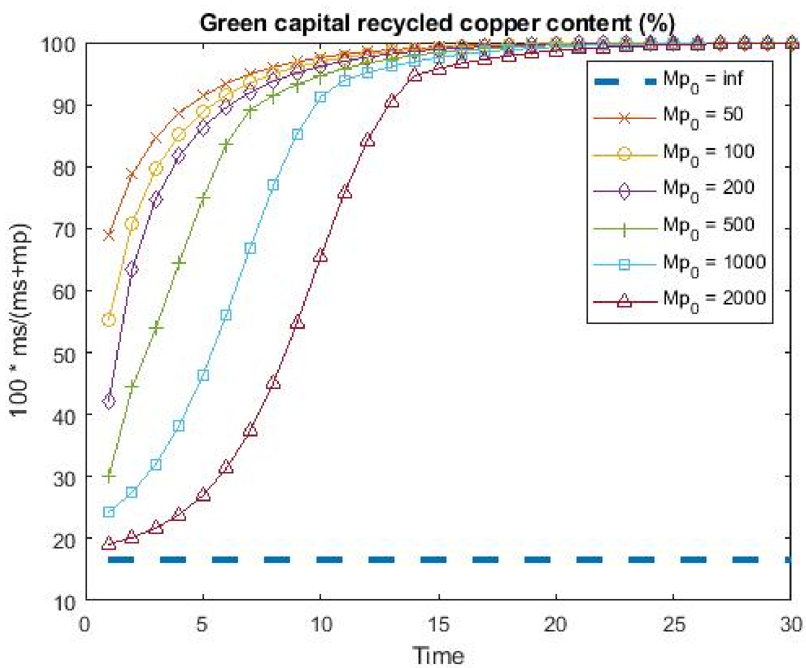

Figure 4: Share of recycled copper in green capital

Result 3 *When primary mineral is abundant, green capital's recycled mineral content is stable at 15%. The slowdown and decline of primary mineral produc-*

tion leads to a gradual increase of recycled mineral share in green capital, until it eventually reaches 100%.

5.4 Labour and green capital inputs to low-carbon energy production

Figure 5 shows the paths of green capital and labour inputs to low-carbon energy production in the $M_{p,t=0} = 1000$ MtCu scenario. Green capital input reaches a peak, but labour input keep increasing thanks to labour productivity gains, in spite of a gradual decline of low-carbon energy labour share. In the long run, the non-substitutability of green capital and labour input limits low-carbon energy production. Labour productivity gains delay by 6-8 decades the low-carbon energy production peak.

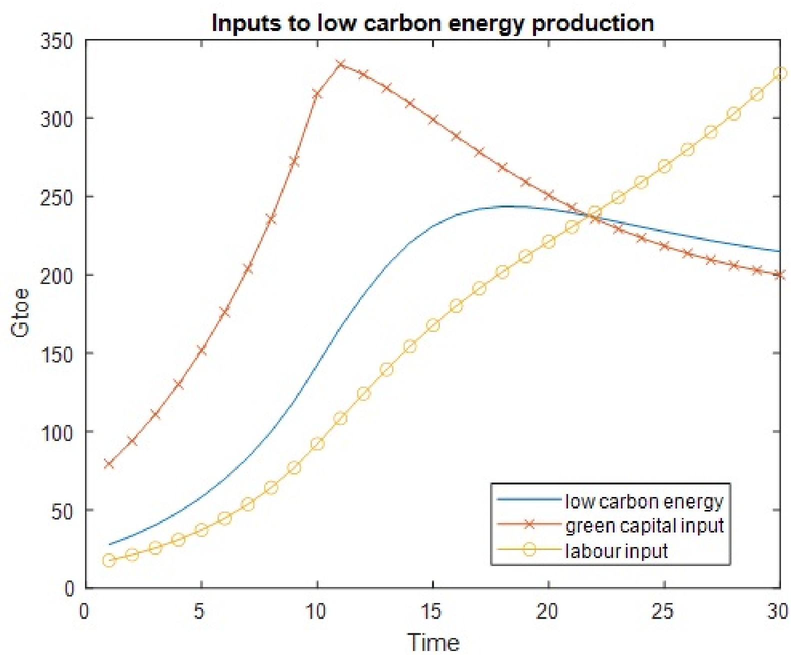

Figure 5: Green capital and labour inputs to low-carbon energy production, for a mineral constraint $M_{p,t=0} = 1000$ MtCu

Result 4 *After the green capital peak, labour productivity gains delay low-carbon energy production peak by 6-8 decades.*

5.5 Key dates in each scenario

The previous sections describe some key steps that occur in every finite mineral scenario, namely:

- primary copper extraction peak
- 100% recycling rate
- low-carbon energy production peak

The date of those events differs according to the magnitude of the mineral constraint. Thus, a higher $M_{p,t=0}$ delays the primary copper peak and the low-carbon energy peaks. This section gives the dates of those events in each scenario.

In order to highlight the growing difference between low-carbon energy production in finite and infinite mineral scenario, we also denote the dates of the following events :

- low-carbon energy production is 10% inferior to the infinite mineral scenario
- low-carbon energy production is 20% inferior to the infinite mineral scenario
- low-carbon energy production is 50% inferior to the infinite mineral scenario
- low-carbon energy production is 66% inferior to the infinite mineral scenario

Table 2 summarizes all those results. Notice that in all scenarios, the low-carbon energy peak coincides with the moment when low-carbon energy production is approximately 2/3 lower than in the infinite mineral scenario. The time unit is 10 years, and time starts in 2010: t=6 refers to an event that happens in 2070. *10% < infty* refers to the moment when low-carbon energy production is 10% lower than in the infinite mineral scenario. Dates are given with a precision of ±0.5 decade.

Table 2: Dates of key events in each scenarios

Mineral constraint (MtCu)	50	100	200	500	1000	2000
Primary copper peak	< 1	< 1	1	3	6	9
100% recycling rate	< 1	< 1	1	7	11	15
10% < infty	< 1	< 1	2	7.9	11.1	15
20% < infty	< 1	< 1	5	9.3	12.7	16.2
50% < infty	3	5.7	8.7	12.8	16.2	19.6
66% < infty	6	8	11	15	18	22
Low-carbon energy peak	6	8	11	15	18	22

5.6 Impact on GDP and optimal carbon tax

In the infinite mineral scenario, low carbon energy production grows unlimited. In all constrained scenarios, it reaches a peak at one point. Since energy are assumed to be non-substitutable, fossile energies can't compensate for this limitation. As a consequence, total available energy for final good production E_t can't follow the infinite mineral scenario path. This engenders a relative loss of GDP compared to the unconstrained scenario.

Figure 6 shows that in all constrained scenarios considered, GDP starts to depart from the infinite mineral scenario path at one point. When comparing with the key dates from Table 2, we observe that GDP drops from the moment when mineral recycling rate as reached its maximum level of 100%, that is for instance at t=7 in the 500Mt primary copper budget scenario. 7 decades after this date, GDP is 1% lower in the constrained scenario. It is 5% lower at the end of the simulation.

As in GHKT, the optimal carbon tax is a stationary ratio of the GDP. Therefore, plotting relative variations of GDP or optimal carbon tax paths is equivalent. Thus, figure 6 also shows how the optimal carbon tax path is changed by the mineral constraint. In constrained scenarios, the optimal carbon tax is 3-8% lower than in the infinite mineral scenario after 30 decades, depending on the mineral constraint considered.

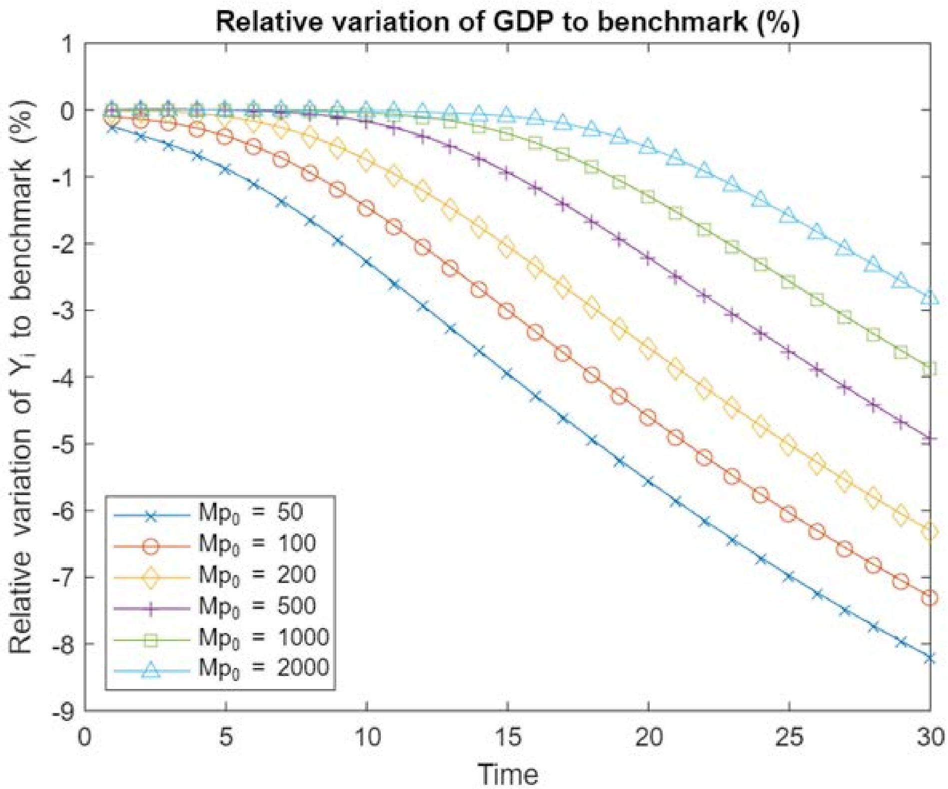

Figure 6: Comparison of GDP with the infinite mineral scenario for various mineral constraints

6 Extension: other low-carbon energy sources

In our model, as in GHKT, low-carbon energy production is aggregated into a single sector, ignoring the diversity of low-carbon energy sources. Nuclear energy and hydroelectricity generation, which currently account for the main part of low-carbon energy production, are not as mineral intensive as solar and wind energy production [10] [25]. While in the long run, solar and wind energy production are expected to be the two main low-carbon energy sources, in the short and medium term, nuclear and hydroelectricity production are non negligible sources of low carbon energy sources. In this section we incorporate these two sources into the production function of low-carbon energy.

In BP energy outlook, nuclear energy and hydroelectricity production growth rate declines gradually, from 1.7% annually between 2010 and 2020, to 0.57% per year between 2030 and 2040. For simplicity, we assume that nuclear energy and hydroelectricity generation is constant to its projected 2040 level during all the simulation. Therefore, the production function for total low-carbon energy becomes :

$$E_{3,t} = (\kappa_L (A_{3,t} N_{3,t})^{\ddot{\rho}} + \kappa_G (\psi G_t)^{\ddot{\rho}})^{\frac{1}{\ddot{\rho}}} + NH, \tag{28}$$

where NH is a constant that denotes nuclear and hydroelectricity production. In this production function, the first term accounts for solar and wind energy, whereas the second term accounts for nuclear and hydroelectricity. Following BP energy outlook [2], we use a decennal nuclear and hydroelectricity production NH = 20 Gtoe .

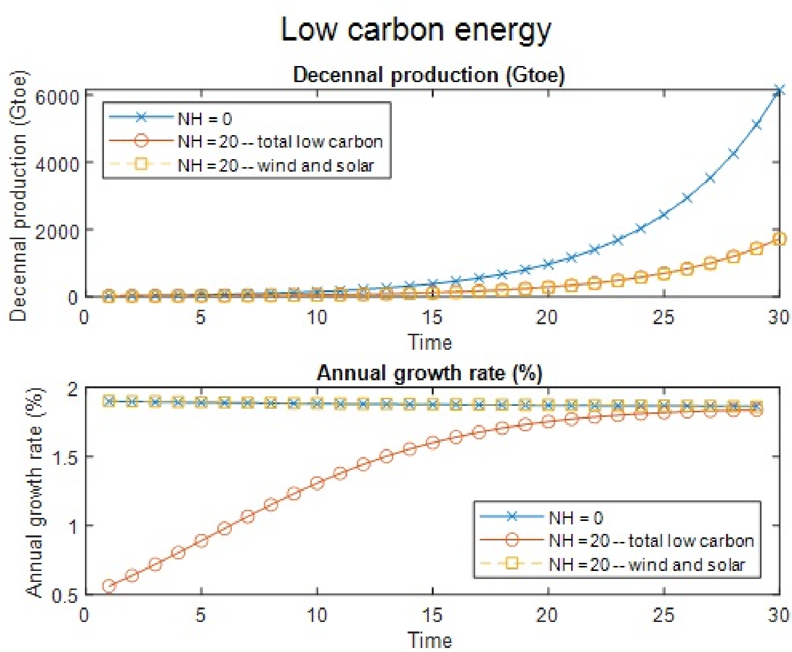

Figure 7: Comparison of low-carbon energy production paths for various values of nuclear and hydroelectricity production

We re-calibrate $A_{3,t=0}$ so that the initial low-carbon energy production matches GHKT. We re-run the simulation in the infinite mineral scenario. We observe that the variable part of low-carbon energy production (solar and wind energy) grows at 1.9% per year, as in the base model. However, this variable part is initially lower than in the base model, so that total low-carbon energy production grows slower in this model than in the base model. The constant term (nuclear and hydroelectricity) quickly becomes negligible with respect to the variable term (solar and wind energy). In the long run, total low-carbon energy grows at the same pace in both models, that is 1.9% per year, but the initial difference induces a 7 decades shift between both paths.

7 Conclusion

Many actors point the key role of minerals in the energy transition. We model the primary and secondary mineral sector response to a booming demand caused by a growing low-carbon energy production. We observe the impact of a mineral constraint on green energy production paths in various mineral scarcity scenarios.

For this purpose, we add to a benchmark energy transition model (Golosov, Hassler, Krussel, and Tsyvinski, 2014) a "green capital" input for renewable energy transition made from primary or recycled minerals. Following GHKT, we use for our simulations a 3 energy sources case (oil, coal and low-carbon energy). We use as a case study the copper input to low-carbon energy production.

When there is an infinite amount of minerals, the result of our model simulation is identical to the benchmark case : our model matches GHKT. When there is a finite amount of mineral, the energy transition paths, and particularly low-carbon energy production, eventually departs from the infinite mineral scenario. We simulate the model's response to various levels of mineral constraint. If the primary copper budget for low-carbon energy green capital is 50 MtCu (which is 20 times the current amount of copper involved in wind energy production worldwide), low-carbon energy production path will be 50% lower than in the infinite mineral scenario in three decades, and will peak in 6 decades. More generally, a doubling (resp. 2-fold division) of the primary copper budget postpones (resp. brings forward) this date by 30 years (±10 years). Along the energy transition, green capital recycled mineral content grows, as a consequence of the combined decline of primary mineral extraction and increase of mineral recycling. When mineral recycling rate reaches 100%, which happens 4

to 6 decades after primary mineral extraction peaks, green capital also peaks. Once green capital's upper bound is reached, low-carbon energy production's growth rate declines. Labour productivity gains notably mitigates the slowdown of low-carbon energy production, but in the long run, low-carbon energy production stabilizes at a plateau, which value depends on the mineral constraint considered.
Our simulations show that the mineral constraint has to be taken into account in energy transition modeling, since it significantly impacts low-carbon energy production paths. It reveals the successive steps that ultimately lead to low-carbon energy production limitation, and gives some insights on the date of those key events for many mineral constraint scenarios.

It is important to note that our analysis offered quantitative results only in the case of one mineral, adding other minerals to the analysis would likely compound the results obtained in this paper in terms of the limitations of low-carbon energy growth. Measuring this impact would be interesting for future investigation. A second natural and desirable future addition consists of including the environmental damages associated with the modified depletion of the minerals implied by the energy transition.

References

[1] D. L. P. Arrobas, K. L. Hund, M. S. Mccormick, J. Ningthoujam, and J. R. Drexhage, *The growing role of minerals and metals for a low carbon future.* World Bank Group, 2017.

[2] British Petroleum, *BP Energy Outlook*, 2019.

[3] Canadian Institue of Mining. (2014) CIM definition standards for mineral resources mineral reserves. [En ligne]. Disponible: https://mrmr.cim.org/en/standards/canadian-mineral-resource-and-mineral-reserve-definitions

[4] Copper Development Association. (2018) Copper in wind power 2. [En ligne]. Disponible: https://copperalliance.org.uk/knowledge-base/education/education-resources/copper-wind-power-2/

[5] Copper Development Association Inc. (2020) Copper in the USA: Bright future glorious past. [En ligne]. Disponible: https://www.copper.org/education/history/us-history/g_fact_future.html

[6] European Commission, *Study on the review of the list of critical raw materials*, 2017.

[7] ——, *Report on critical raw materials and the circular economy*, 2018.

[8] A. García-Olivares, J. Ballabrera-Poy, E. García-Ladona, and A. Turiel, "A global renewable mix with proven technologies and common materials," *Energy Policy*, vol. 41, pp. 561–574, 2012.

[9] M. Golosov, J. Hassler, P. Krusell, and A. Tsyvinski, "Optimal taxes on fossil fuel in general equilibrium," *Econometrica*, vol. 82, no. 1, pp. 41–88, 2014.

[10] E. G. Hertwich, T. Gibon, E. A. Bouman, A. Arvesen, S. Suh, G. A. Heath, J. D. Bergesen, A. Ramirez, M. I. Vega, and L. Shi, "Integrated life-cycle assessment of electricity-supply scenarios confirms global environmental benefit of low-carbon technologies," *Proceedings of the National Academy of Sciences*, vol. 112, no. 20, pp. 6277–6282, 2015.

[11] International Copper Study Group. (2020) Copper: Preliminary data for october 2019. [En ligne]. Disponible: https://www.icsg.org/index.php/component/jdownloads/finish/114/2993?Itemid=

[12] International Council on Mining and Metals, *The role of mining in national economies*, 2014.

[13] International Renewable Energy Agency, *Renewable Energy Cost Analysis - Wind Power*, 2012.

[14] K. M. Johnson, J. M. Hammarstrom, M. L. Zientek, and C. L. Dicken, "Estimate of undiscovered copper resources of the world, 2013," *US Geological Survey Fact Sheet*, vol. 3004, p. 2014, 2014.

[15] M. Knoblach, M. Roessler, and P. Zwerschke, "The elasticity of substitution between capital and labour in the US economy: A meta-regression analysis," *Oxford Bulletin of Economics and Statistics*, vol. 82, no. 1, pp. 62–82, 2020.

[16] L. D. Meinert, G. R. Robinson, and N. T. Nassar, "Mineral resources: Reserves, peak production and the future," *Resources*, vol. 5, no. 1, p. 14, 2016.

[17] National Resources Canada. (2019) Copper facts. [En ligne]. Disponible: https://www.nrcan.gc.ca/our-natural-resources/minerals-mining/minerals-metals-facts/copper-facts/20506

[18] S. Northey, S. Mohr, G. M. Mudd, Z. Weng, and D. Giurco, "Modelling future copper ore grade decline based on a detailed assessment of copper resources and mining," *Resources, Conservation and Recycling*, vol. 83, pp. 190–201, 2014.

[19] G. Pitron, *La guerre des métaux rares. La face cachée de la transition énergétique et numérique.* Les Liens qui Libèrent, 2018.

[20] N. Rötzer and M. Schmidt, "Decreasing metal ore grades—is the fear of resource depletion justified?" *Resources*, vol. 7, no. 4, p. 88, 2018.

[21] United Nations Environmental Program, *Critical Metals for Future Sustainable Technologies and their Recycling Potential*, 2009.

[22] US Department of Energy, *Critical Materials Strategy*, 2011.

[23] US Geological Survey, "Assessment of undiscovered deposits of gold, silver, copper, lead, and zinc in the united states," *US Geological Survey Circular 1178*, p. 19, 1998.

[24] O. Vidal, B. Goffé, and N. Arndt, "Metals for a low-carbon society," *Nature Geoscience*, vol. 6, no. 11, p. 894, 2013.

[25] O. Vidal, F. Rostom, C. François, and G. Giraud, "Global trends in metal consumption and supply: the raw material–energy nexus," *Elements: An International Magazine of Mineralogy, Geochemistry, and Petrology*, vol. 13, no. 5, pp. 319–324, 2017.

A Calibration

Table 3: Calibration summary

Parameter	Interpretation	Calibration condition	Value	Unit
$\kappa_s, \kappa_p, \tilde{\rho}$	Production function of green capital – substitution and share parameters of primary and secondary mineral inputs	▪ $\kappa_s + \kappa_p = 1$ ▪ $\frac{\kappa_s}{\kappa_p}(\frac{m_{s,t=0}}{m_{p,t=0}})^{\tilde{\rho}-1} = 1$ ▪ $\tilde{\rho} = 0.5$	▪ $\kappa_s = 0.3085$ ▪ $\kappa_p = 0.6915$ ▪ $\tilde{\rho} = 0.5$	-
$A_{p,t=0}, A_{s,t=0}$	Initial labour productivity in primary and secondary mineral production sectors	▪ $\frac{(1-\alpha-\nu)Y_{t=0}}{A_{p,t=0}} = 3.5e^9$ ▪ $\frac{(1-\alpha-\nu)Y_{t=0}}{A_{s,t=0}} = 3.5e^9$	▪ $A_{p,t=0} = 132000$ ▪ $A_{s,t=0} = 132000$	$\frac{MtCu}{Labour}$
ψ	Amount of energy produced (over the course of one period) for 1 unit of green capital	▪ $\frac{G_{t=0}}{E_{3,t=0}} = 4\ tCu/MW$	▪ $\psi = 1.877$	$\frac{Gtoe}{Labour}$
$\kappa_G, \kappa_L, \ddot{\rho}$	Green energy production function– substitution and share parameters of labour and green capital inputs	▪ $\kappa_G + \kappa_L = 1$ ▪ $\frac{\kappa_L}{\kappa_G}(\frac{A_{3,t=0}N_{3,t=0}}{\psi G_{t=0}})^{\ddot{\rho}-1} = \frac{1}{3}$ ▪ $\ddot{\rho} = -3$	▪ $\kappa_G = 0.75$ ▪ $\kappa_L = 0.25$ ▪ $\ddot{\rho} = -3$	-
$A_{3,t=0}$	Initial labour productivity in green energy sector	▪ $F(A_{3,t=0}, A_{s,t=0}, A_{p,t=0}) = 1311$	▪ $A_{3,t=0} = 865.14$	$\frac{Gtoe}{Labour}$
g_{A3}, g_{As}, g_{Ap}	Growth rate of labour productivities	▪ $g_{A3}, g_{As}, g_{Ap} = 1.02^{10}$	▪ $g_{A3}, g_{As}, g_{Ap} = 1.02^{10}$	-
$M_{s,t=0}, M_{p,t=0}$	Initial primary and secondary mineral stocks	▪ $M_{s,t=0} = 19\ MtCu$	▪ $M_{s,t=0} = 19$ ▪ $M_{p,t=0} = 500, 1000, 2000, 5000, 10000, 20000, 50000$	$MtCu$

Table 3 summarizes all the parameter choices and equations used for the calibration. The following paragraphs provide sources and details about the calibration.

$\boldsymbol{\kappa_s}$, $\boldsymbol{\kappa_p}$, $\boldsymbol{\tilde{\rho}}$ are the parameters of the green capital CES production function. The relative price of primary mineral to recycled mineral is one [5]. Current primary and recycled copper production is given in [11]. On the one hand, copper is 100% recyclable and does not degrades in the process, so that primary and secondary copper can equivalently be used [17], which suggests a high substitution parameter. On the other hand, if primary and secondary copper were perfect substitutes, the simulation would lead to situations where only the current cheapest industry is active at a time, which is not what is observed in reality, where primary and secondary copper industries coexists. Therefore, we choose a very high substitution parameter, but strictly lower than one. $\tilde{\rho} = 0.5$ is our guess. The choice of this parameter has an impact on the difference between the peak low-carbon energy production, and the long run plateau low-carbon energy production. The better substitutes primary and secondary mineral are, the lower the difference. In the limit, if primary and secondary mineral are perfect substitutes ($\tilde{\rho} = 1$), green energy production in the long run is equal to peak production.

$\boldsymbol{A_{p,t=0}}$, $\boldsymbol{A_{s,t=0}}$. Primary copper production cost is estimated to 3500\$/tCu [12]. We don't have an estimate for secondary copper production cost, but good quality scrap copper is currently worth 3400\$/tCu. For simplicity, we assume that the total production cost of secondary copper is 3500\$/tCu (including capital and labour cost).

$\boldsymbol{\psi}$ is the amount of wind energy produced over the course of one period for each unit of green capital. It depends on the technology, and especially the location of the wind turbine. Garcia-Olivares (2012) estimates that onshore wind turbines needs 2 tons of copper per MW installed, whereas offshore wind turbines need 10 tons per MW [8]. Copper Development Association's estimation is 2.4 - 6.5 t/MW [4]. We use 4t/MW in order to take into account both onshore and offshore wind turbines, since offshore wind turbines are expected to have a growing role in the future of wind energy production.

$\boldsymbol{\kappa_G}$, $\boldsymbol{\kappa_L}$, $\boldsymbol{\ddot{\rho}}$ characterize the substitution between labour and green capital input in wind energy production. Labour cost share over capital cost share in wind energy production varies from one country to another, but it is around 1 to 3 on average: labour represents 25% of wind energy production cost, and capital 75% [13]. Knoblach et al. (2020) metastudy estimates that the elasticity of substitution between labour and capital is between 0.45 and 0.87 at the most aggregated level, and that it is 0.2 points lower at the industry level [15]. We take the lowest value of the interval, assuming that green capital is not easily substituted by labor. Therefore, we get an elasticity of substitution of 0.25, which gives a substitution parameter of -3. Arguing that green capital and labour are bad substitutes, we approximate labour input to green capital input ratio to one. With this assumption, we simplify table 3 equation to $\frac{\kappa_L}{\kappa_G} = \frac{1}{3}$. This leads to $\kappa_L = 0.25$. This result states that wind energy production is more capital intensive than labour intensive.

$\boldsymbol{A_{3,t=0}}$. We use proposition (3) to calibrate $A_{3,t=0}$

$\boldsymbol{g_{A3}}$, $\boldsymbol{g_{As}}$, $\boldsymbol{g_{Ap}}$. Following GHKT, we assume an annual 2% labour productivity growth rate in each sector.

$\boldsymbol{M_{s,t=0}}$. We assume that the initial secondary mineral stock corresponds to one year of current primary copper production, that is 19Mt copper.

B Proof of Proposition 1

B.1 Equation (19)

This result also holds in GHKT's model; we enhance that the modifications and additions that are specific to our model keep this result and its proof unchanged.

We combine the first order conditions with respect to $N_{0,t}$ and $N_{2,t}$ to obtain the following equality :

$$\lambda_{0,t} \frac{\partial Y_t}{\partial N_{0,t}} = \lambda_{2,t} \frac{\partial E_{2,t}}{\partial N_{2,t}}.$$

Then, the first order conditions with respect to $E_{2,t}$, E_t and S_t give an expression of coal's marginal production cost $\lambda_{2,t}$:

$$\lambda_{2,t} = \lambda_{0,t}\frac{\partial Y_t}{\partial E_t}\frac{\partial E_t}{\partial E_{2,t}} - \lambda_{0,t}\Lambda_t,$$

where the expression of the marginal climate externality damage Λ_t is identical to GHKT. We replace in the first equality $\lambda_{2,t}$ by its expression to obtain result 19.

B.2 Equation (20)

Since we use a new production function for low-carbon energy production (that includes green capital), equation (20) differs from GHKT's result, but the proof is analog.

We combine the first order conditions with respect to $N_{0,t}$ and $N_{3,t}$ to obtain the following equality :

$$\lambda_{0,t}\frac{\partial Y_t}{\partial N_{0,t}} = \lambda_{3,t}\frac{\partial E_{3,t}}{\partial N_{3,t}}.$$

Then, we obtain from the first order conditions with respect to $E_{3,t}$ and E_t that

$$\lambda_{3,t} = \lambda_{0,t}\frac{\partial Y_t}{\partial E_t}\frac{\partial E_t}{\partial E_{3,t}},$$

which leads immediately to result (20).

B.3 Equation (21)

Equation (21) is specific to our model, since there is no secondary mineral sector in GHKT.

We combine the first order conditions with respect to $N_{0,t}$ and $N_{s,t}$ to obtain :

$$\lambda_{0,t}\frac{\partial Y_t}{\partial N_{0,t}} = \lambda_{s,t}\frac{\partial m_{s,t}}{\partial N_{s,t}}.$$

Then, we get from the first order conditions with respect to $m_{s,t}$ and G_t that :

$$\lambda_{s,t} = \lambda_{3,t}\frac{\partial E_{3,t}}{\partial G_t}\frac{\partial G_t}{\partial m_{s,t}}.$$

Using the intermediate result from the proof of equation (20), we obtain :

$$\lambda_{s,t} = \lambda_{0,t} \frac{\partial Y_t}{\partial E_t} \frac{\partial E_t}{\partial E_{3,t}} \frac{\partial E_{3,t}}{\partial G_t} \frac{\partial G_t}{\partial m_{s,t}},$$

which leads to result (21).

C Proof of Proposition 2

C.1 Equation (22)

Equation (22) and its proof are identical as in GHKT.

The first order conditions with respect to $E_{1,t}$, E_t, and S_t gives

$$\mu_{1,t} = U'(C_t) \frac{\partial Y_t}{\partial E_t} \frac{\partial E_t}{\partial E_{1,t}} + \frac{1}{\beta^t} \sum_{j=t}^{T} U'(C_j) \frac{\partial Y_j}{\partial S_j} \frac{\partial S_j}{\partial E_{1,t}} \tag{29}$$

For readability purposes, denote by A_t the first term in the right-hand side of equation (29), and B_t the second term. Then,

$$\mu_{1,t} = A_t + B_t,$$

where $\mu_{1,t}$ is the Lagrange multiplier that stands for oil's scarcity cost.

The first order condition with respect to $R_{1,t+1}$ gives a necessary condition on the evolution of the Lagrange multiplier over time :

$$\mu_{1,t} = \beta \mu_{1,t+1} \tag{30}$$

A_t is the contribution of $E_{1,t}$ to final good consumption. Using equations (1), (4) and (5), it becomes :

$$A_t = -\frac{Y_t}{C_t} \frac{\nu \kappa_1}{E_t^{\rho} E_{1,t}^{1-\rho}}$$

B_t accounts for all the present and future damages induced by a present carbon emission $E_{1,t}$.

Using equations (4) and (9), we obtain

$$\text{for all } j > t, \quad \frac{\partial Y_j}{\partial S_j} \frac{\partial S_j}{\partial E_{1,t}} = -\gamma_j Y_j \ (1 + d_{j-t}).$$

Therefore, B_t can be written, after a variable change :

$$B_t = \sum_{j=0}^{T-t} \beta^j \gamma_{t+j} \frac{Y_{t+j}}{C_{t+j}} (1 - d_j).$$

Define

$$\hat{\Lambda}_t = \sum_{j=0}^{T-t} \beta^j \gamma_{t+j} (1 - d_j).$$

Using GHKT's result that the optimal saving rate is constant over time, B_t becomes

$$B_t = \hat{\Lambda}_t \, \frac{Y_t}{C_t}.$$

Finally, when replacing $\mu_{1,t}$ and $\mu_{1,t+1}$ by their expression in equation (30), we obtain result (22).

C.2 Equation (23)

The first order condition with respect to $m_{p,t}$ is

$$\lambda_{p,t} + \mu_{p,t} - \mu_{s,t} - \pi_{G,t} \frac{\partial G_t}{\partial m_{p,t}} = 0.$$

The first order conditions with respect to $N_{p,t}$ and $N_{0,t}$ give :

$$\chi_t^N - \lambda_{p,t} \frac{\partial m_{p,t}}{\partial N_{p,t}} = 0$$
$$\chi_t^N - \lambda_{0,t} \frac{\partial Y_t}{\partial N_{0,t}} = 0.$$

Therefore,

$$\begin{aligned} \lambda_{p,t} &= \lambda_{0,t} \frac{\partial Y_t / \partial N_{0,t}}{\partial m_{p,t} / \partial N_{p,t}} \\ &= \frac{Y_t}{C_t} \frac{1 - \alpha - \nu}{A_{p,t} N_{0,t}}. \end{aligned}$$

We now have an expression of $\lambda_{p,t}$. Then, consecutively substituting Lagrange multiplier by their expressions obtained from the first order conditions with respect to G_t, $E_{3,t}$, E_t, E_t^0 one obtains

$$\pi_{G,t} = U'(C_t) \cdot \frac{\partial Y_t}{\partial E_t^0} \cdot \frac{\partial E_t}{\partial E_{3,t}} \cdot \frac{\partial E_{3,t}}{\partial G_t}.$$

Finally, the first order conditions with respect to $M_{p,t+1}$ and $M_{s,t+1}$ give:

$$\mu_{p,t} - \beta\mu_{p,t+1} = 0$$
$$\mu_{s,t} - \beta\mu_{s,t+1} = 0,$$

so that

$$\mu_{p,t} - \mu_{s,t} = \beta(\mu_{p,t+1} - \mu_{s,t+1}).$$

In the end, we obtain equation (23).

D Proof of proposition 3

This section provides detail on the analytical resolution of the infinite mineral case. We prove that under some conditions, the infinite mineral case in our modelling is equivalent to GHKT's model. We first aim to express green capital G_t as a function of labour shares $N_{p,t}$ and $N_{s,t}$.

Assume that $M_{p,t=0} = \infty$, $M_{s,t=0} = \infty$, and $g_{As} = g_{Ap} = g_{A3}$. The first order condition with respect to $m_{p,t}$ can be written:

$$\lambda_{p,t} + \mu_{p,t} - \mu_{s,t} - \pi_{G,t}\frac{\partial G_t}{\partial m_{p,t}} = 0.$$

However, since the primary and secondary mineral stocks are infinite, mineral scarcity rents $\mu_{p,t}$ and $\mu_{s,t}$ are equal to zero. Therefore,

$$\lambda_{p,t} = \pi_{G,t}\frac{\partial G_t}{\partial m_{p,t}}. \quad (33)$$

Moreover, the first order condition with respect to $N_{p,t}$ gives :

$$-\lambda_{p,t}\frac{\partial m_{p,t}}{\partial N_{p,t}} + \chi_t^N = 0,$$

and the first order condition with respect to $N_{0,t}$ gives :

$$-\lambda_{0,t}\frac{\partial Y_t}{\partial N_{0,t}} + \chi_t^N = 0,$$

so that we have

$$\lambda_{p,t}\frac{\partial m_{p,t}}{\partial N_{p,t}} = \lambda_{0,t}\frac{\partial Y_t}{\partial N_{0,t}}. \tag{34}$$

We combine equations 33 and 34 to obtain :

$$\pi_{G,t}\frac{\partial G_t}{\partial m_{p,t}}\frac{\partial m_{p,t}}{\partial N_{p,t}} = \lambda_{0,t}\frac{\partial Y_t}{\partial N_{0,t}}. \tag{35}$$

We repeat the same process with the secondary mineral flow variables $m_{s,t}$ and $N_{s,t}$. The first order condition with respect to $m_{s,t}$ gives :

$$\lambda_{s,t} = \pi_{G,t}\frac{\partial G_t}{\partial m_{s,t}},$$

and the first order conditions with respect to $N_{s,t}$ and $N_{0,t}$ lead to :

$$\lambda_{s,t}\frac{\partial m_{s,t}}{\partial N_{s,t}} = \lambda_{0,t}\frac{\partial Y_t}{\partial N_{0,t}},$$

so that

$$\pi_{G,t}\frac{\partial G_t}{\partial m_{s,t}}\frac{\partial m_{s,t}}{\partial N_{s,t}} = \lambda_{0,t}\frac{\partial Y_t}{\partial N_{0,t}}. \tag{36}$$

We combine equations 35 and 36:

$$\frac{\partial G_t}{\partial m_{s,t}}\frac{\partial m_{s,t}}{\partial N_{s,t}} = \frac{\partial G_t}{\partial m_{p,t}}\frac{\partial m_{p,t}}{\partial N_{p,t}}. \tag{37}$$

Equation 37 states that labour's marginal contribution to green capital manufacturing in primary and secondary mineral sectors are equal. It extends Proposition 1 result and is only valid when primary and secondary mineral stocks are infinite. Equation 37 can now be written using the formula that define G_t as a function of $m_{p,t}$ and $m_{s,t}$:

$$\kappa_p A_{p,t}\left(\frac{G_t}{m_{p,t}}\right)^{1-\tilde{\rho}} = \kappa_s A_{s,t}\left(\frac{G_t}{m_{s,t}}\right)^{1-\tilde{\rho}},$$

which leads to

$$\frac{N_{p,t}}{N_{s,t}} = \frac{A_{s,t}}{A_{p,t}} \left(\frac{\kappa_p A_{p,t}}{\kappa_s A_{s,t}} \right)^{\frac{1}{1-\tilde{\rho}}}.$$

Denote by α_1 the primary to secondary mineral labour shares ratio :

$$\alpha_1 = \frac{A_{s,t}}{A_{p,t}} \left(\frac{\kappa_p A_{p,t}}{\kappa_s A_{s,t}} \right)^{\frac{1}{1-\tilde{\rho}}}.$$

We write the expression of G_t using α_1 :

$$G_t = \left(\kappa_s \left(A_{s,t} \frac{1}{1+\alpha_1} \right)^{\tilde{\rho}} + \kappa_p \left(A_{p,t} \frac{\alpha_1}{1+\alpha_1} \right)^{\tilde{\rho}} \right)^{\frac{1}{\tilde{\rho}}} (N_{p,t} + N_{s,t}),$$

and define the aggregated green capital labour productivity

$$\widehat{A}_{G,t} = \left(\kappa_s \left(A_{s,t} \frac{1}{1+\alpha_1} \right)^{\tilde{\rho}} + \kappa_p \left(A_{p,t} \frac{\alpha_1}{1+\alpha_1} \right)^{\tilde{\rho}} \right)^{\frac{1}{\tilde{\rho}}},$$

so that

$$G_t = \widehat{A}_{G,t} \, (N_{p,t} + N_{s,t}). \tag{38}$$

Equation 38 expresses green capital as a function of primary and secondary labour shares, using the aggregated green capital labour productivity $\widehat{A}_{G,t}$. This result is only valid when mineral stocks are infinite.

Using the intermediate result of equation 38, the following steps aim to express low-carbon energy production $E_{3,t}$ as a function of labour shares $N_{p,t}$, $N_{s,t}$ and $N_{3,t}$. Combine equations 20 and 21 to obtain that low-carbon energy labour and secondary mineral labour's marginal contribution to low-carbon energy production are equal :

$$\frac{\partial E_{3,t}}{\partial N_{3,t}} = \frac{\partial E_{3,t}}{\partial G_t} \frac{\partial G_t}{\partial N_{s,t}}. \tag{39}$$

In equation 39, we replace $E_{3,t}$ and G_t by their expression :

$$\kappa_L A_{3,t} \left(\frac{E_{3,t}}{A_{3,t} N_{3,t}} \right)^{1-\ddot{\rho}} = \kappa_G \psi \widehat{A}_{G,t} \left(\frac{E_{3,t}}{\psi G_t} \right)^{1-\ddot{\rho}},$$

which leads, using equation 38, to :

$$\frac{N_{3,t}}{N_{s,t}+N_{p,t}} = \frac{\psi \widehat{A}_{G,t}}{A_{3,t}} \left(\frac{\kappa_L A_{3,t}}{\kappa_G \psi \widehat{A}_{G,t}} \right)^{\frac{1}{1-\ddot{\rho}}}$$

Denote by α_2 the direct to indirect low-carbon energy labour ratio:

$$\alpha_2 = \frac{\psi \widehat{A}_{G,t}}{A_{3,t}} \left(\frac{\kappa_L A_{3,t}}{\kappa_G \psi \widehat{A}_{G,t}} \right)^{\frac{1}{1-\ddot{\rho}}}.$$

We write the expression of $E_{3,t}$ using α_2:

$$E_{3,t} = \left(\kappa_L \left(A_{3,t} \frac{\alpha_2}{1+\alpha_2} \right)^{\ddot{\rho}} + \kappa_G \left(\psi \widehat{A}_{G,t} \frac{1}{1+\alpha_2} \right)^{\ddot{\rho}} \right)^{\frac{1}{\ddot{\rho}}} (N_{3,t} + N_{p,t} + N_{s,t})$$

and define the aggregated low-carbon energy labour productivity

$$\widehat{A}_{3,t} = \left(\kappa_L \left(A_{3,t} \frac{\alpha_2}{1+\alpha_2} \right)^{\ddot{\rho}} + \kappa_G \left(\psi \widehat{A}_{G,t} \frac{1}{1+\alpha_2} \right)^{\ddot{\rho}} \right)^{\frac{1}{\ddot{\rho}}},$$

so that

$$E_{3,t} = \widehat{A}_{3,t} \ (N_{s,t} + N_{p,t} + N_{3,t}). \tag{40}$$

Equation 40 expresses low-carbon energy as a function of labour shares of all sectors that are involved in low-carbon energy production. Thus, when primary and secondary mineral stocks are infinite, low-carbon energy production function can be written in a form that is analog to GHKT's low-carbon energy production function. Assume now that the aggregated labour productivity $\widehat{A}_{3,t}$ has the same initial value and growth-rate than GHKT's low-carbon energy labour productivity. Then, our model is mathematically equivalent to GHKT's model.